Structural Considerations in Case II Swelling of Crystalline Poly(ethylene Terephthalate)

TOSHIO HAGA, *Faculty of Education, Hirosaki University, Hirosaki-City, Aomori 036, Japan*

Synopsis

The Case II swelling in chloroform was discussed with regard to the fine structure for the crystalline PET. The case II swelling was associated with the character of the crystallites. It was inferred that the fine structure related to the Case II behavior was effectively plasticized during the swelling process.

INTRODUCTION

The Case II swelling[1] in which the solvent uptake increases linearly with time has been often reported for amorphous, glassy polymers.[2-6] The author recently developed the appearance of the Case II behavior in solvents for the crystalline PET.[7-9]

The driving force for the Case II swelling was taken as the stress gradient of the solvent within the polymer.[10] The stress may develop through the chemical potential difference of the solvent between the swollen and unswollen parts.[11] There is a sharp boundary separating the outer swollen shell from the inner unswollen core for the Case II swelling.[1] Sarti[11] evaluated the above stress in terms of the osmotic pressure. It was considered that the osmotic pressure is exerted on the pure polymer in order to compensate the chemical potential decrease in the swollen polymer due to the solvent presence.[11]

Diffusion behavior of the solvent is well recognized to depend upon the fine structure with regard to the crystalline polymer. It was reported[9] that the diffusion coefficient and the penetration velocity, characterizing the Case II swelling rate, is remarkably influenced by the presence of the crystalline region.

In the present paper, it is shown that the osmotic pressure causing the Case II behavior in chloroform is closely associated with the character of the crystallites for PET. The fine structure of PET related the Case II swelling together with the plasticizing effect of the solvent on the swelling mechanism was also discussed.

EXPERIMENTAL

Materials

Unoriented PET film of crystallinity 10.6% and the thickness 350 μm was used as a starting material for the preparation of the samples having different crystallinity. This film was offered by Teijin Co., Ltd. PET film of crystallinity 5.3% and thickness 30 μm was obtained from the above film using a melt-

Journal of Applied Polymer Science, Vol. 27, 2653–2661 (1982)
 CCC 0021-8995/82/072653-09$01.90

quenching technique and was used to prepare the films for the IR measurements. The oriented PET fiber was 75D/12f and offered by Toray Industry Inc. The solvents used were reagent grade.

Crystallization Methods

The crystallization and the annealing were carried out in the silicone oil. After the specified length of time at a given temperature, the film was taken out of the bath and then put in ice water for quenching.

For the melt-crystallization, the film was molten at 280°C for 5 min in the silicone oil followed by the crystallization at 240°C for the time ranging from 10 to 300 min. In the case of the crystallization from the glass, the crystallization was employed for each 30°C rise in temperature from 120°C to 240°C. The crystallization time was 1 h for the films other than that, having the largest degree of crystallinity in this category for which the time is 5 h.

The annealing was undergone at 240°C for 6 h on the films crystallized from the glass at 120°C and 180°C for 1 h. The crystallization by solvents was run to achieve the equilibrium crystallinity at room temperature.

Swelling Measurements

A solvent uptake Q_t was obtained as described before.[9]

Crystallinity Measurements

Crystallinity X_c was obtained by a density method.[9]

The PET film crystallized by solvents was recognized to have a abnormally low density due to the presence of the extensive voids generated at the desorption of the solvents.[12] In this case, the practical density which is not influenced by the extensive voids was employed to calculate the crystallinity. The practical value of density was obtained through the measurements of Statton's crystallinity index.[13] That is, the value was established by a combination of the crystallinity index for the solvent-crystallized PET and the linear relationship between the density and the crystallinity index for the PET crystallized from the glass.[14]

IR Measurements

IR-A3 infrared spectrometer manufactured by Japan Spectroscopic Co., Ltd., was used to analyze PET. The amount of regular fold R_I was obtained as the ratio of the absorption intensity at 988 cm^{-1} band to that at 795 cm^{-1} band.[15] The base lines for 988 cm^{-1} and 795 cm^{-1} bands were drawn by means of Prevorsek's[16] and Schmidt's[17] methods, respectively. The Koenig's procedure[15] using the AgCl plate was taken up for the measurements of the melt-crystallized film.

X-Ray Measurements

Wide angle X-ray diffraction patterns were recorded using a Rigaku Geigerflex instrument with nickel-filtered CuKα radiation.

DSC Measurements

Rigaku 8001SLC differential scanning calorimeter was used for the measurements. Heating rate is 2.5°C/min. The sample amount of 3 mg was measured under a stream of nitrogen.

Calculation of the Osmotic Pressure

Osmotic pressure π was calculated in terms of the following equation which was used by Sarti[11]:

$$\pi = (RT/V_1)[v_1 - \chi_1 v_1^2 - (1/X)\ln(1 - v_1)] \quad (1)$$

where V_1 is the molar volume of solvent, v_1 is the volume fraction of solvent in the PET–solvent mixture, χ_1 is the Flory–Huggins interaction parameter, X is the molar volume ratio of solvent to polymer, and R and T represent gas constant and absolute temperature, respectively.

It is reasonably assumed that $1/X$ is nearly zero, such that the expression (1) reduces to

$$\pi = (RT/V_1)(v_1 - \chi_1 v_1^2) \quad (2)$$

Practical calculation was done using expression (2). v_1 was calculated using $Q_\infty/(1 - X_c)$, the equilibrium uptake in the amorphous region.

χ_1 between chloroform—PET was not known so far. Therefore, it was roughly evaluated as 1.12 through the application of the Flory–Huggins equation to the equilibrium sorption of chloroform into the amorphous region of the PET fiber.[18] The solvent concentration is uniform within the swollen layer when the swelling process obeys the Case II behavior.[1] The concentration within the swollen layer for this mechanism was assumed to be equal to the equilibrium sorption Q_∞.

The extensive void may only apparently increase Q_∞. Therefore, the corrected equilibrium value excluding the void content v was obtained by the equation:

$$\frac{d_p}{1 + v/(1 - v)} = d_a \quad (3)$$

where d_p is the practical value of density, as described before, and d_a is the apparent value of density, respectively.

RESULTS AND DISCUSSION

Effect of the Character of the Crystallites

Swelling behavior in chloroform at 50°C and X_c as well as the osmotic pressure for the PET films crystallized by various methods are shown in Table I. $Q_\infty/(1 - X_c)$ is assumed to be the equilibrium swelling in the amorphous region, while Q_∞ exhibits the apparent value for the bulk film including the unpenetrable crystalline region.

Samples with various crystallinity are obtained by means of the change of the crystallization time for the isothermal crystallization from the melt. In the case of that from the glass, X_c becomes over a wide range by changing both the temperature and the time.

Within the limit of each crystallization method, the swelling mechanism

TABLE I
Swelling Characteristics in Chloroform and Crystallinity for PET Films Crystallized by Various Methods.

No.	Crystallization condition	Crystallinity X_c (%)	Equilibrium swelling Q_∞ (%)	Osmotic pressure π (atm)	Swelling mechanism
1	Isothermally	13.9	29.2		Fickian
2	Crystallized	53.1	15.2		Fickian
3	From the melt	61.9	14.6		Fickian + Case II
4		65.8	12.2	61.6	Case II
5		69.2	10.5	59.9	Case II
6	Isothermally	42.6	34.8		Fickian
7	Crystallized	48.5	25.9		Fickian + Case II
8	From the glass	52.5	21.2		Fickian + Case II
9		58.3	19.5		Fickian + Case II
10		66.4	14.3		Fickian + Case II
11		70.2	14.7	68.8	Case II
	Crystallization				
	By solvents				
12	By acetone	51.5	35.7		Fickian + Case II
13	By methyl ethyl ketone	51.0	41.7		Fickian + Case II
14	By chloroform	53.6	33.3 (31.9)[a]	73.5	Case II
	Annealed				
15	Starting material: 6	74.7	13.2	69.8	Case II
16	Starting material: 8	73.7	14.8	70.8	Case II

[a] The value freed of effect of the extensive void content.

changes from the Fickian to the Case II behavior with an increase in X_c and much nearly with an decrease in Q_∞. This is not correct all over X_c and Q_∞ beyond the crystallization method.

Focussing on the PET in which the Case II behavior appears, the osmotic pressure is minimum for the melt-crystallized film and maximum for the solvent-crystallized film. Further, the PET crystallized from the glass exhibits a slightly smaller pressure than that annealed.

It is well known that the structural properties of the crystallite are different according to the crystallization method. R_I/X_c was estimated as a structural parameter of the crystallites in this study. A thermodynamically stable crystallite is well recognized to be in connection with a larger amount of regular fold especially for the unoriented polymer as examined in this study. R_I/X_c together with R_I are shown in Table II only for the films which exhibit the Case II mechanism.

R_I/X_c as well as R_I are much smaller for the solvent-crystallized PET 14. This observation is consistent with that by Lawton and Cates.[12] The maximum R_I and R_I/X_c appears for the melt-crystallized sample 5. It is probable that more complete crystallites were grown during the melt-crystallized process at 240°C.

It has been recognized that the crystallites are well grown at a much higher treating temperature[19,20] such as 240°C for the samples 5, 11, and 15. 240°C is well above the glass transition temperature and is near to the melting temperature for PET. However, since the original glassy material has a definite degree of crystallinity, the crystallites for the PET crystallized from the glass 11 seem to take a lower completeness than for the melt-crystallized PET 5 in which the starting material is completely amorphous. It is believed that the presence of the crystallites would hinder the formation of a heavily perfect crystallite due to the limitation of diffusion of the polymer segment.

The annealing of a isothermally crystallized PET above the crystallization temperature results in increased thermal stability of the crystalline structure.[21] Nevertheless, the structure of the annealed sample differs considerably from that obtained by direct isothermal crystallization from the amorphous state.[21] The regular lamellar structures are not well grown in the former case.[21]

The starting material of the annealed sample 15 is of crystallinity 42.6%. This suggests that the segmental motion of the polymer chain would be strongly hindered and that the structural transformation upon the annealing would be insufficient. It is reasonable that the crystal completeness for the annealed PET 15 is more poor than for the melt-crystallized PET 5.

It is certain that the chloroform-crystallized PET exhibits the most poor

TABLE II
Relative Amount of Regular Fold R_I and That Related to Crystalline Region R_I/X_c in PET Films Exhibiting Case II Swelling in Chloroform.

No.[a]	R_I	R_I/X_c
5	0.370	0.535
11	0.275	0.392
14	0.064	0.119
15	0.326	0.436

[a] Numbers refer to the films noted in Table I.

completeness of the crystallites among the samples indicated in Table II. Wide-angle X-ray patterns of films 5, 11, 14, and 15 are shown in Figure 1. The patterns unexceptionally indicate the reflections based upon the crystalline region. The reflections developed for the sample 14 appears much broader than that for samples 11 and 15. In addition, the reflections for the sample 5 is fairly more sharp than that for samples 11 and 15. The sharpening of the reflections is ascribed to the crystal completeness. Therefore, the qualitative evaluations of the patterns supports the description based upon IR measurements.

DSC measurements reveal that the melting peaks for samples 5 and 14 are 255.5°C and 253.5°C, respectively. This observation is also in excellent agreement with that established by IR measurements.

The plots of R_I/X_c against the osmotic pressure related to the Case II swelling are shown in Figure 2. R_I/X_c decreases with an increase in the osmotic pressure. The result suggests that the Case II swelling is closely connected with the completeness of the crystallites.

Hoffman and Week's equation[22] dealing with the melting behavior of the crystallite indicates that a thermodynamically stable crystallite has a larger la-

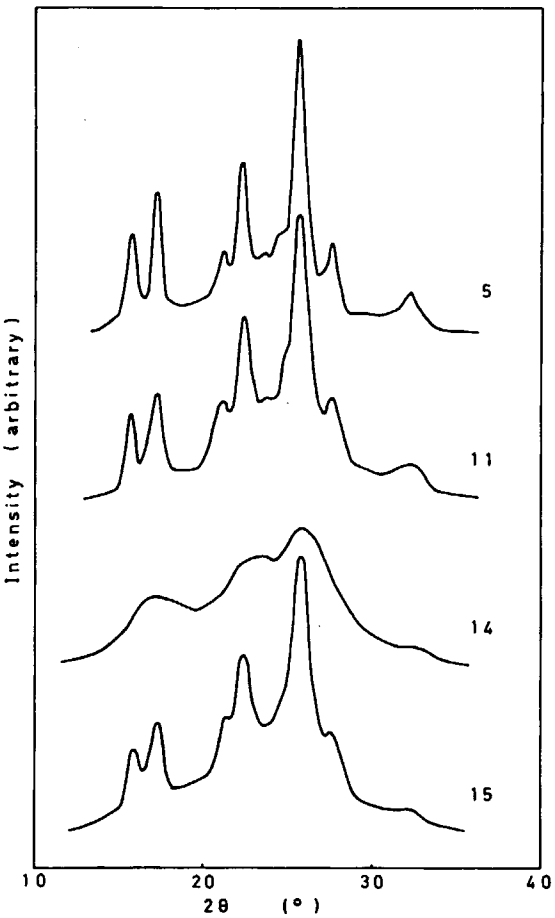

Fig. 1. Wide angle X-ray patterns of the PET films prepared by various crystallization conditions indicated in Table I.

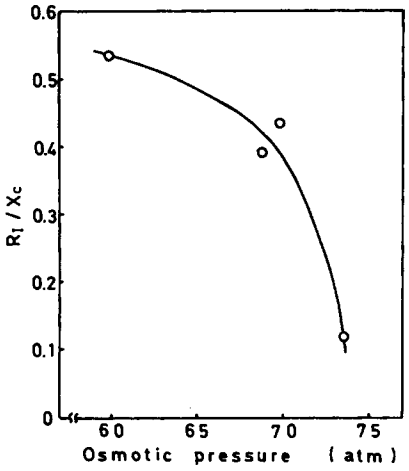

Fig. 2. Relative amount of regular fold related to the crystalline region R_I/X_c vs. osmotic pressure at which the Case II behavior appears in chloroform for the PET films crystallized by various methods.

mellar thickness. Also, a sharpening of the X-ray reflections is interpreted in terms of an increase in the crystal size together with an improvement of the crystalline order.[23]

Figure 1 relating to the X-ray reflections indicates that the reflections developed for sample 11 is more sharp than that for sample 15. This observation is rather definitely consistent with the result of the osmotic pressure associated with the Case II behavior. Although quantitative X-ray measurements to obtain the crystal size were not performed here, one possibility of the description may be attributed to the fact that the crystal size plays a very important role in the appearance of the Case II mechanism.

Consequently, it may be concluded that the Case II behavior occurs at a lower osmotic pressure for the film in which the crystallites are well known. Although the sorption may occur in the amorphous region alone, the Case II mechanism is closely associated with the crystalline parts.

Plasticizing Effect of Solvents for the Appearance of the Case II Behavior

The swelling under the fixed condition was compared with that under the relaxed condition for the PET fiber. The measurements were carried out at 10°C. The plots of ln Q_t against ln t (t = swelling time) are shown in Figure 3. The slope of the plots represents the value of the exponent n for the following equation:

$$Q_t = kt^n \tag{4}$$

where k is a constant. n is known to characterize the swelling mechanism.[24] Case II swelling is manifested by $n = 1$, while the Fickian mechanism results in $n = 0.5$. The Fickian + Case II behavior seems to indicate a intermediate value of n.

The swelling process under the fixed condition represents $n = 1$ and obeys the Case II mechanism. For the relaxed condition, $n = 0.9$ was calculated from the

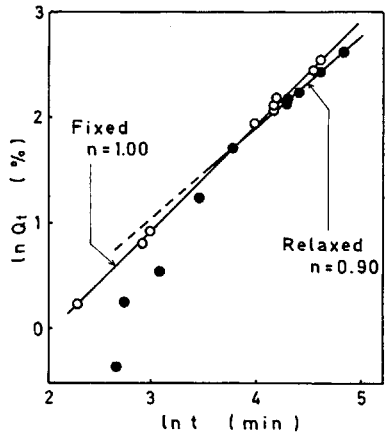

Fig. 3. The ln Q_t against ln t plots in chloroform for the PET fibers under the fixed and relaxed conditions at 10°C. n indicates the slope of the linear plots and the exponent for eq. (4). (○) Under the fixed condition; (●) under the relaxed condition.

linear relationship which appeared except at the initial step of swelling. The deviation from the linearity at the initial step was also observed in the plot of $Q_t/t^{1/2}$ against $t^{1/2}$. This deviation is often observed in the intermediate swelling mechanism for the PET—solvent system, as reported previously.[9]

It is assumed that the Case II contribution to the swelling process may increase due to the constraint of the amorphous chain. This constraint may involve the prevention of the extention in the direction of the radius, since the shrinkage in the direction of the fiber axis could be hardly observed due to the presence of the unswollen core, especially at the initial stage of swelling.[25]

Apparent activation energy for swelling[9] under the fixed condition is 20.9 kcal/mol, while being 24.1 kcal/mol under the relaxed condition. The author previously examined the activation energy of swelling for the annealed PET fiber and showed that the magnitude of the activation energy change with the annealing was smaller for PET, which had a tendency to exhibit the Case II behavior.[18,20] It is probable that the mobility of the amorphous chain was enhanced due to the effective plasticization during the Case II process.

It has been found that the structure in connection with the Case II behavior exhibits more elastic character for PET.[14] This may indicate the relaxation time of the molecular chain for the structure is rather infinitely long. The molecular chain which has a extremely short or long relaxation time may be responsible for the appearance of the Fickian sorption.[24] In contrast, the Case II behavior seems to develop when the polymer relaxation and the solvent diffusion rates are comparable.[24]

From these discussions, it can be assumed that the molecular chain of the crystalline PET related to the Case II behavior has a essentially long relaxation time itself. Also, because of the plasticization during the swelling process, the relaxation of the relevant chain is considered to fall within the intermediate range responsible for the appearance of the Case II behavior.

CONCLUSION

The swelling in chloroform for the PET films crystallized from various methods was examined. The swelling mechanism was strictly associated with the fine

structure for PET. It was found that the Case II behavior appeared at a smaller osmotic pressure for the PET which had thermodynamically stable crystallites. Although the sorption seems to occur in the amorphous region alone, the swelling mechanism is closely connected with the structural parameter concerning the crystalline region.

The stress was assumed to take an important role in the appearance of the Case II behavior for the crystalline PET as well as for the amorphous polymer. It was evidenced that the fine structure related to the Case II behavior was effectively plasticized during the swelling process.

The author is grateful to Professor S. Yui for the use of the X-ray diffractometer.

References

1. T. Alfrey, Jr., E. F. Gurnee, and W. G. Lloid, *J. Polym. Sci.*, **C12**, 249 (1966).
2. A. S. Michaels, H. J. Bixler, and H. B. Hopfenberg, *J. Appl. Polym. Sci.*, **12**, 991 (1968).
3. C. H. M. Jacques, H. B. Hopfenberg, and V. Stannet, *Polym. Eng. Sci.*, **14**, 441 (1974).
4. T. K. Kwei and H. M. Zupko, *J. Polym. Sci., Part A-2*, **7**, 867 (1969).
5. T. K. Kwei, T. T. Wang, and H. M. Zupko, *Macromolecules*, **5**, 645 (1972).
6. H. B. Hopfenberg, L. Nicolais, and E. Drioli, *Polymer*, **17**, 195 (1976).
7. T. Haga and H. Ishibashi, *Seni-Gakkaishi*, **29**, T-489 (1973).
8. T. Haga, *Seni-Gakkaishi*, **34**, T-145 (1978).
9. T. Haga, *J. Appl. Polym. Sci.*, **26**, 2649 (1981).
10. H. L. Frisch, T. T. Wang, and T. K. Kwei, *J. Polym. Sci., Part A-2*, **7**, 879 (1969).
11. G. C. Sarti, *Polymer*, **20**, 827 (1979).
12. E. L. Lawton and D. M. Cates, *J. Appl. Polym. Sci.*, **13**, 899 (1969).
13. W. O. Statton, *J. Appl. Polym. Sci.*, **7**, 803 (1963).
14. T. Haga, *Seni-Gakkaishi*, **34**, T-360 (1978).
15. J. L. Koenig and M. L. Hannon, *J. Macromol. Sci. (Phys.)*, **B1**, 119 (1967).
16. D. C. Prevorsek, G. A. Tirpak, P. J. Harget, and A. C. Reimschuessel, *J. Macromol. Sci.-Phys.*, **B9**, 733 (1974).
17. P. J. Schmidt, *J. Polym. Sci., Part A*, **1**, 1271 (1963).
18. T. Haga, thesis, Tokyo Institute of Technology, 1981.
19. N. C. Watkins and D. Hansen, *Text. Res. J.*, **38**, 388 (1968).
20. G. Groeninckx, H. Berghmans, and G. Smets, *J. Polym. Sci. Polym. Phys. Ed.*, **14**, 591 (1976).
21. G. Groeninx and H. Reynaers, *J. Polym. Sci., Polym. Phys. Ed.*, **18**, 1325 (1980).
22. J. D. Hoffman and J. J. Weeks, *J. Res. N. B. S.*, **66A**, 13 (1962).
23. L. E. Alexander, *X-ray Diffraction Methods in Polymer Science*, Wiley, New York, 1969.
24. H. B. Hopfenberg, R. H. Holley, and V. Stannet, *Polym. Eng. Sci.*, **9**, 242 (1969).
25. A. S. Ribnick, H.-D. Weigmann, and L. Rebenfeld, *Text. Res. J.*, **43**, 123 (1973).
26. T. Haga and H. Ishibashi, *Seni-Gakkaishi*, **29**, T-489 (1973).

Received July 14, 1981
Accepted January 28, 1982